Research Article

Fiammetta Venuti*

Influence of pattern anisotropy on the structural behaviour of free-edge single-layer gridshells**

https://doi.org/10.1515/cls-2021-0011
Received Sep 15, 2020; accepted Dec 19, 2020

Abstract: Free-edge gridshells represent the majority of built gridshells. Indeed, the gridshell reference geometry usually needs to be trimmed in order to provide building access or to insert the gridshell within an existing building, giving rise to one or more elastic boundaries. Despite the current design practice, so far a very limited number of scientific studies has been devoted to investigate the influence of elastic boundaries on the overall structural behaviour of gridshells. This paper focuses on the effects of the orientation of the boundary structure with respect to the grid direction. This is done by studying the buckling behaviour of an ideal single-layer steel gridshell, for different grid layout (quadrangular, hybrid, triangular) and orientation. The results of the parametric study demonstrate that the sensitivity of free-edge single-layer gridshells to the free-edge orientation strongly depends on the grid pattern. In particular, isotropic gridshells have shown an almost negligible influence of the free-edge orientation in terms of buckling load, in opposition to orthotropic gridshells. Moreover, the change in free-edge orientation induces significant variations of the global structural stiffness for all the layouts, resulting in possibly unacceptable displacements in service conditions.

Keywords: single-layer gridshell, free-edge, anisotropy, grid pattern, buckling

1 Introduction

Gridshells belong to the family of lightweight form-resistant structures [1], together with tensegrity structures [2, 3] and cable and membrane structures [4]. They are designed to cover large spans and optimised to ideally bear loads by means of in-plane internal forces. Since the pioneering structure designed by Shukov [5] at the end of the 19th century, gridshell design has evolved through the master works of Buckminster Fuller [6], Frei Otto [7] and Schlaich Bergermann und Partner [8, 9], resulting in a huge number of built structures all over the world [9–11].

Gridshell structures are highly prone to buckling phenomena, as testified by catastrophic collapses such as the one of the Bucharest Exhibition Hall dome in 1963. Since then, a lot of research has been devoted to the buckling behaviour of these kind of structures (for a review see *e.g.* Ref.s [12, 13]).

The buckling behaviour of gridshells is influenced by several factors [12, 13], such as Gaussian curvature of the reference surface [12, 14, 15], grid topology and spacing [16–19], imperfections [14, 20–22], stiffness of the joints [20, 23–25] and boundary conditions [12, 14]. All the cited studies have been carried out by referring to gridshells with horizontal spring-plane and rigid supports. Surprisingly, gridshells of this kind represent a minority and are limited to research pavilions [7, 26] - horizontally constrained at the ground level - or roofs - rigidly constrained along their perimeter to the underlying structure - such as the Neckarsulm dome [8] or the British Museum Great Court roof [27]. In the majority of built gridshells, the complete gridshell surface has been trimmed due to functional or architectural reasons, giving rise to free-edges at the intersection between the reference geometry and the trimming surface. Outstanding examples of this kind are the Multihalle in Mannheim [28], whose reference surface is trimmed by vertical planes to provide access; the Hippo House at the Berlin Zoo [29], cut by a curved surface; the Cabot Circus in Bristol [30], where cuts are made to insert the gridshell within an existing building. Despite the current design practice, "this kind of elastic boundary has not been extensively investigated, and studies are needed in each design to know how and if the supports improve the buckling resistance" [13].

A first attempt to systematically study the stability of free-edge gridshells has been performed by Venuti and Bruno [31]. Here, free-edge gridshells are named Partial

***Corresponding Author: Fiammetta Venuti:** Department of Architecture and Design, Polytechnic of Turin, Viale Mattioli 39, I-10125, Torino, Italy; Email: fiammetta.venuti@polito.it

** Paper included in the Special Issue entitled: Shell and Spatial Structures: Between New Developments and Historical Aspects

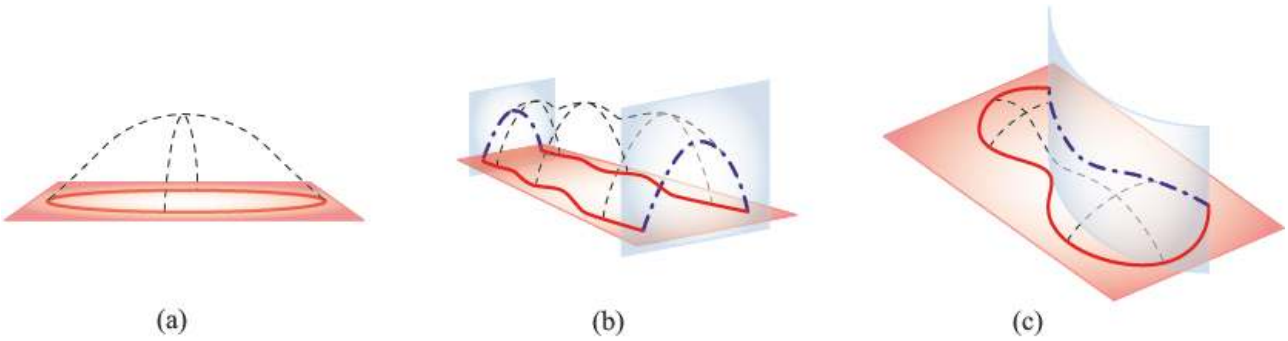

Figure 1: Definition of CG (a) and PG cut by vertical planes (b) and curved surface (c) (after Venuti and Bruno [31])

Gridshells (PG) in opposition to Complete Gridshells (CG). In the latter case, the shape derives from a reference geometry trimmed by a single surface (Figure 1a): the structure is rigidly constrained along the boundary given by the intersection between the reference and the trimming surfaces. In the case of PGs, the reference geometry is trimmed by more than one trimming surface, giving rise to one rigid boundary (usually the ones which lies horizontally) and one or more elastic boundaries (Figure 1b-c). The cited authors studied the influence of mechanical factors on the stability of PGs. Specifically, the effects of the flexural stiffness of the elastic boundaries and of the in-plane shear stiffness of the gridshell were explored on an ideal hybrid single-layer steel gridshell dome. The results of the study showed that, depending on the ratio between stiffness of the boundary and in-plane stiffness of the gridshell, the structural buckling behaviour could be free-edge driven or shell-driven.

This paper aims at carrying on the study by starting to investigate the influence of geometrical factors on the buckling behaviour of free-edge gridshells. Specifically, the stability of PGs is expected to also depend on the kind of trimming surface (either planar or curved), its orientation with respect to the grid direction and its location (*i.e.* the ratio between the free-edge and the gridshell spans). This study will focus on the effects of anisotropy, *i.e.* of different orientation of the trimming plane with respect to the grid direction. It will be carried out through a parametric study on an ideal free-edge gridshell dome by considering different grid layouts.

The paper outline is as follows: first, the parametric study is described in terms of geometrical and structural set ups and kind of structural analyses adopted to evaluate the buckling behaviour; then, results are discussed in terms of buckling loads and shapes and interpreted on the basis of the grid pattern classification; finally, conclusions and research perspectives are summarised in the last section.

2 Parametric analysis set-up

2.1 Geometrical set-up

The reference geometry of the investigated free-edge single-layer gridshell is shown in Figure 2. The analytical form of the reference continuous dome (Figure 2a) is a paraboloid, having a parabola as both the directrix and generatrix (red and blue curves in Figure 2a). The considered free-edge dome is obtained by trimming the complete dome with a vertical plane Ω passing through the origin of the reference system and rotated of an angle θ with respect to the $y - z$ plane. The obtained half dome is, therefore, bounded by a vertical parabolic arch, whose geometrical parameters are: span length $L = 30$ m, span to rise ratio $L/f = 8$. The discrete gridshell geometry results from the point wise sampling of the dome surface in P structural nodes ($p = 1, P$) along the directions of the directrix and generatrix. The nodes are connected along the directions of the directrix and generatrix by straight segments resulting in elemental planar quads [29], having a characteristic length $l \approx 1.5$ m (Figure 3a).

In order to study the effects of the grid anisotropy with respect to the gridshell free-edge, four different orientations of the Ω plane are considered, corresponding to angle θ of 0°, 15°, 30° and 45°, respectively (Figure 2b).

Moreover, the sensitivity to anisotropy of gridshells having different grid topology is also investigated. To do so, for each value of θ three kinds of grid layout are considered:

1. quadrangular (Q) (Figure 3a);
2. hybrid (H) (Figure 3b), where the quad meshes are stiffened by bracing cables [8];
3. triangular (T) (Figure 3c), where the original quad mesh is triangularised by the addition of diagonal elements with the same cross section as the straight ones.

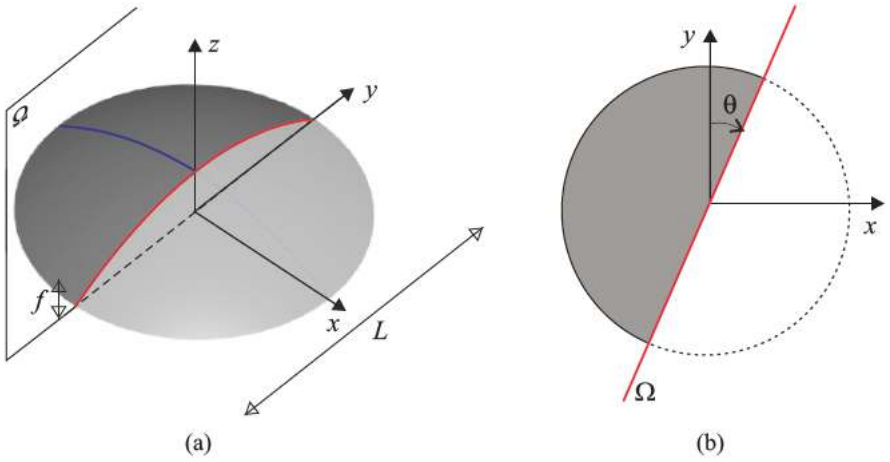

Figure 2: Continuous reference surface: axonometric view (a) and plan view (b)

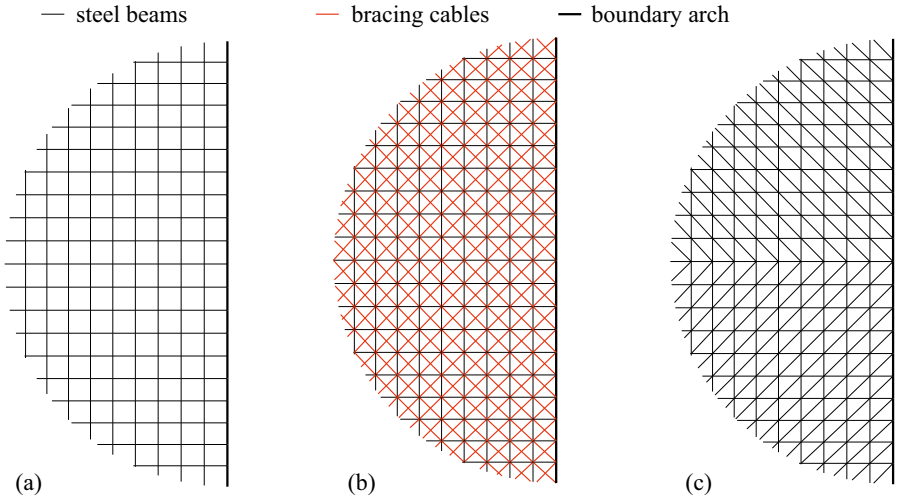

Figure 3: Gridshell layouts: quadrangular (a), hybrid (b) and triangular (c)

2.2 Structural set-up

In all the layouts the main grid is composed of steel beams. Both the grid beam, the bracing cable cross section and the type of joint mimic the one usually adopted in Ref.s [8, 14]: a solid quadrilateral cross section with area $A_e = 2.5 \cdot 10^{-3}$ m^2 is chosen for the steel beams, while the bracing cables have a circular cross section with area equal to $1.6 \cdot 10^{-4}$ m^2 and prestress $\sigma_0 = 100$ MPa. The boundary arch has a solid quadrilateral cross section, whose moment of inertia is 100 times greater than the grid beam one: this value has been chosen based on the free-edge gridshell survey in Ref. [31], where the ratio between the boundary arch and grid beam inertia is reported to typically fall in the range 80-250 for single-layer bending-inactive gridshells.

The structures are covered with glass panels, which are taken into account as dead loads only. The dead load q_d of structural steel members and of 20 mm-thick glass glazing is set equal to 0.5 kN/m^2. A uniform load case $q = 1.3q_d + 1.5q_s$ is applied to the structure according to the Ultimate Limite State load combination, where q_s=0.75 kN/m^2 is the snow load. The resultant p-th nodal load is defined as $Q_p = \int_A q da$, being A the tributary area of the p-th node.

The structure is modelled by means of the finite element software ANSYS® v19.2. Both the grid elements and the boundary arch are modelled in ANSYS using the BEAM188 finite element. The 3D beam elements are based on Timoshenko's beam theory and adopt a cubic shape function. The cables are modelled by 3D unilateral (tension-only) hinged-hinged bar elements with circular cross section (LINK180 finite element). The whole structure is assumed to be hinged at the boundaries, while the joints between steel bars are modelled as rigid, as usually done in the literature [14, 16, 32]. Even though the stiffness of the nodal connections affects the buckling behaviour of this

kind of structures, a more refined model to account for the actual stiffness of the joints has not been introduced since it is not expected to change the results of a comparative study.

The constitutive model of the steel is linear elastic – perfect plastic, with a yield strength equal to $f_y = 355$ MPa, Young's modulus $E = 2.1e + 5$ MPa and Poisson's ratio $\nu = 0.3$.

3 Structural analyses

The buckling loads are calculated by means of three types of analyses [13]: Linear Buckling Analysis (LBA); Geometrically and Materially Nonlinear Analysis (GMNA) on the gridshell without imperfections; Geometrically and Materially Nonlinear Analysis (GMNIA) on the gridshell with imperfections. In GMNIA the distribution of the nodal geometrical imperfections is assumed equal to the first buckling shape obtained through LBA, with maximum imperfection amplitude equal to $L/300$, as suggested in the Chinese code [33].

The structural analysis is performed by means of the finite-element code ANSYS® v19.2. The Load Control procedure is applied within nonlinear analysis, where the iterative convergence is accomplished at each step by means of the standard Newton Raphson method.

The results of the numerical simulations are compared in terms of Load Factor (LF) and buckling shapes. In LBA, the LF can be defined as the ratio between the buckling load Q_u and the reference load Q as defined in the previous section. Within GMNA, the Load factor is defined as the load multiplier corresponding to the limit point in the load-displacement curve ($dQ/d\delta = 0$ in a selected reference node) and $\boldsymbol{\delta}_u$ is the corresponding displacement field.

4 Classification of the grid pattern

Differently from continuous shells, gridshells are characterised by an intrinsic anisotropy, given by the fact that the discrete grid intersects its boundaries (either rigid or elastic) with orientations that can differ from those of the main grid directions. Besides this, a second kind of anisotropy, that we can call *pattern anisotropy*, related to the topology of the grid pattern, can be identified.

In view of the subsequent interpretation of the results, it can be useful to classify the adopted grid patterns with respect to the pattern anisotropy. In physics, anisotropy is the property of being directionally dependent, which implies different properties in different directions, as opposed to isotropy. Orthotropy is a subset of anisotropy and is characterised by properties that differ along three mutually-orthogonal twofold axes of rotational symmetry. When dealing with gridshells, the distinction between isotropic and orthotropic pattern is not straightforward and unanimously accepted in the scientific community and different criteria can be adopted. Some authors adopt a geometrical criterion and consider isotropic all the patterns with equilateral cells: according to this criterion, not only equilateral triangular, but also quad and hybrid meshes are isotropic [34]. Pietroni *et al.* [35] adopt a static criterion and define anisotropic the grid whose elements are aligned with the principal stresses of the underlying surface. Winslow *et al.* [36], on the basis of the continuum analogy, compute the homogenised stiffness matrix of the gridshell unit cell in the case of a triangular grid and obtain the properties of an equivalent anisotropic material. Tonelli *et al.* [18] classify equilateral triangular and hexagon meshes as isotropic and quad meshes as orthotropic. This classification also coincides with the one usually adopted when dealing with grid-stiffened panels [37], which are usually divided into isogrid panels – stiffened by equilateral triangular ribs – and orthogrid panels – stiffened by quadrangular ribs. The same classification is obtained by Mesnil *et al.* [19] through a criterion based on the continuum analogy, which will be adopted in the following. Specifically, they propose to classify the quality of a pattern by calculating the structural efficiency for increasing refinement of the mesh and interpreting the results according to homogenisation principles.

The structural efficiency is defined as the ratio between the buckling load q_{cr}, evaluated by means of LBA, and the weight of the structure [17, 19]:

$$\eta = \frac{q_{cr} \cdot A}{m \cdot g}, \tag{1}$$

where $q_{cr} = q \cdot \mathrm{LF}$, $A = \pi L^2/4$ is the horizontal surface covered by the dome, m is the structural mass and g the gravity acceleration.

The buckling load of a spherical shell dome with uniform pressure is considered for reference. This does not perfectly coincide with the analysed case study – paraboloid dome with vertical distributed load – but it can be considered as a good approximation. The linear buckling load of an equivalent spherical isotropic shell under uniform pressure is proportional to $\sqrt{\mathcal{A}\mathcal{D}}$ [38], where $\mathcal{A}$ and $\mathcal{D}$ are the equivalent shell axial and bending stiffness, respectively. Whichever the grid pattern, $\mathcal{A}$ is a function of EA/l and $\mathcal{D}$ a function of EI/l [13, 38], being A and I the area and moment of inertia of the main grid elements, respectively. Therefore, both the buckling load and the mass m

linearly depends on $1/l$, *i.e.* on the number of cells along the main span L/l, meaning that η is expected to converge to a constant value. On the contrary, the buckling load of an equivalent orthotropic shell is a function of $\sqrt{\mathcal{D}\mathcal{G}}$, where $\mathcal{G}$ is the in-plane shear stiffness and depends on EI/l^3 [13, 19]. Therefore, in this case the buckling load is proportional to $1/l^2$, making η linearly dependent on the number of cells along the main span.

The convergence study is performed on the complete dome, in order to exclude the edge effects induced by the free boundary. Figure 4 plots the structural efficiency for increasing number of cells for each grid pattern. It can be observed that the quad pattern structural efficiency linearly increases for increasing number of cells along the main span $n = L/l$. On the contrary, the triangular pattern has an almost constant structural efficiency when the number of cells exceeds 20. The hybrid pattern shows an intermediate trend, which is expected to depend on the cable axial stiffness.

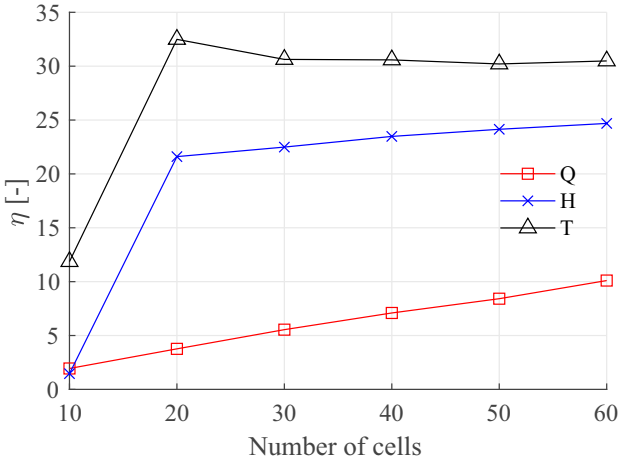

Figure 4: Structural efficiency η versus grid refinement for each grid pattern

On the basis of the above considerations, it can be concluded that the considered triangular gridshell is isotropic, even though the triangles are not equilateral, while the quadrilateral one is orthotropic (in accordance with Mesnil *et al.* [19]). The behaviour of the hybrid gridshell adopted as case study is more similar to the triangular one, therefore it can be classified as isotropic, but it is expected that orthotropic behaviour could emerge for lower values of the cable axial stiffness.

It is worth noting that, on the basis of the modelling assumption made in Section 2.2, the structural mass does not include the one due to the actual dimensions of the nodal connections. This added mass is expected to have increasing influence for increasing number of cells, so that the denominator in Eq. 1 takes larger values for increasing number of nodal connections, potentially leading to different trends of the structural efficiency versus n.

5 Results

In this Section, the results of the parametric analysis are illustrated. First, the influence of the design variable θ on LFs and buckling shapes is commented on. Then, a deeper insight into the mechanical behaviour is provided through the concept of Structural Eigen-Curves [39].

5.1 Load Factors and buckling shapes versus θ

Figure 5 illustrates the LFs as a function of θ, obtained from each structural analysis for each gridshell layout. The results confirm some expected general trends:

- the linear buckling load, obtained through LBA, is higher than the elastic-plastic buckling load, obtained through GMNA [13]. Moreover, the LFs of the imperfect structure are lower than the ones of the perfect structure;
- for each structural analysis and θ, the LFs show an increasing trend from Q to H to T gridshell, due to increasing stiffness of the mesh.

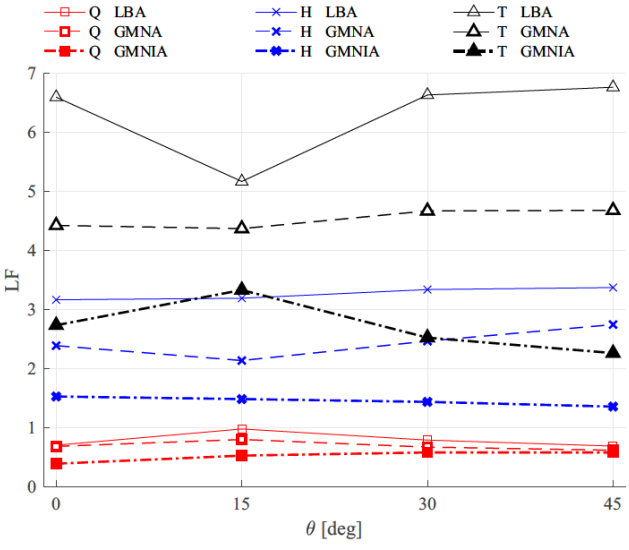

Figure 5: Load Factors obtained from LBA, GMNA and GMNIA for each gridshell layout

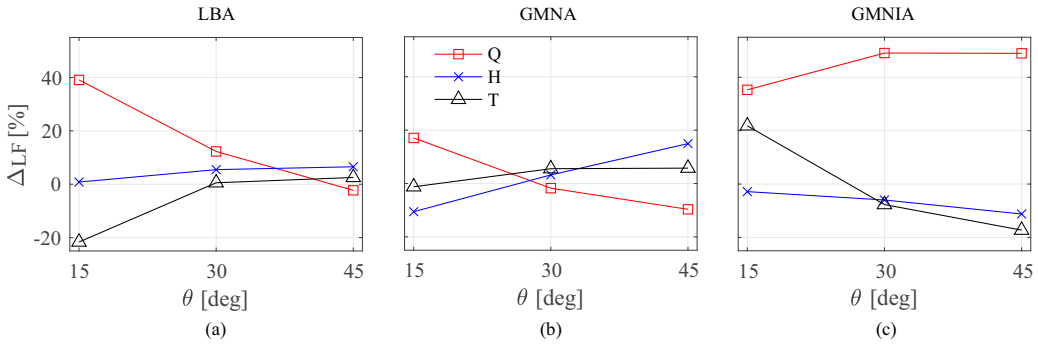

Figure 6: Percentage variation of the Load Factors ΔLF obtained from (a) LBA, (b) GMNA and (c) GMNIA for each gridshell layout

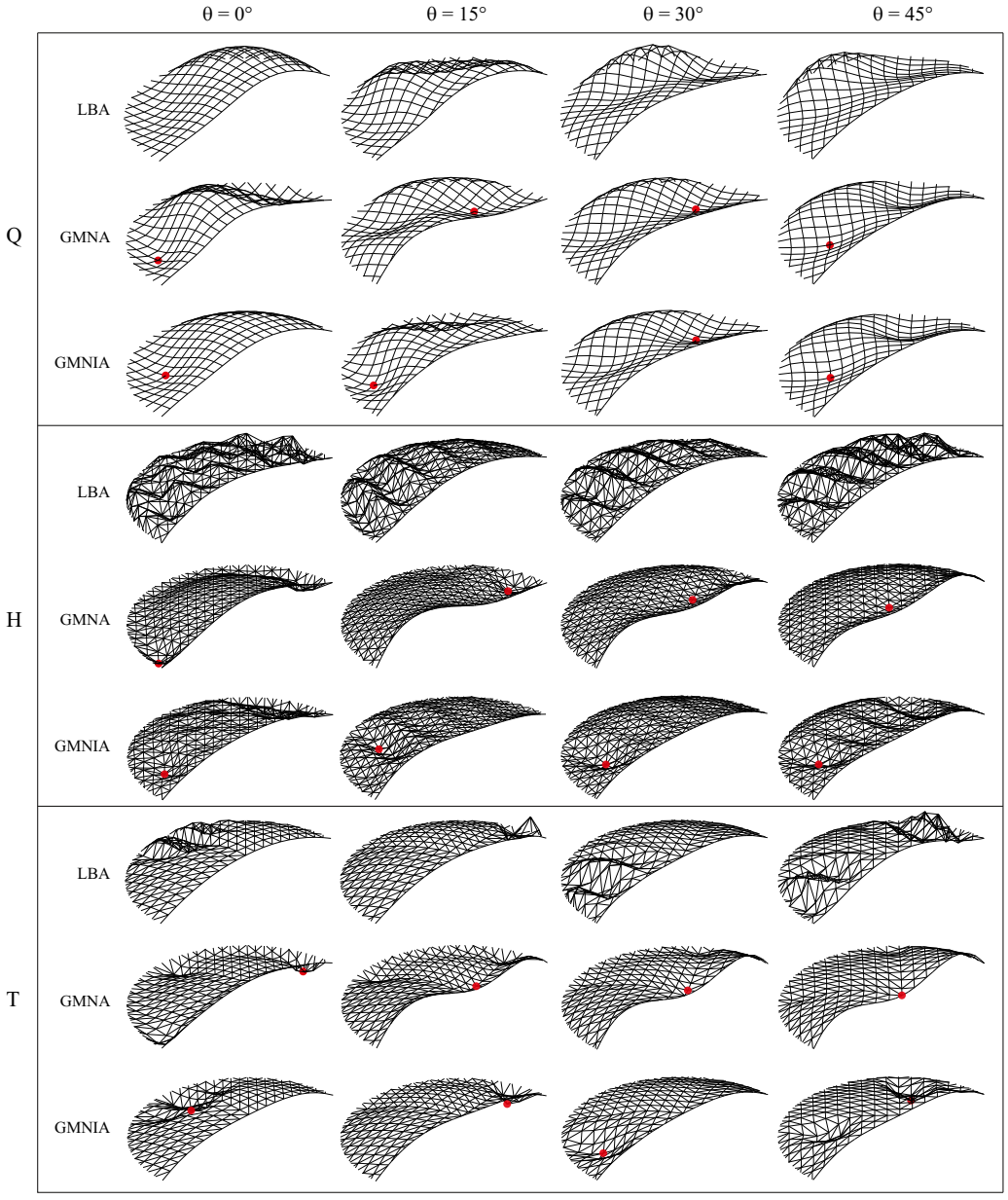

Figure 7: Buckling shapes (displacements normalised to 2 m)

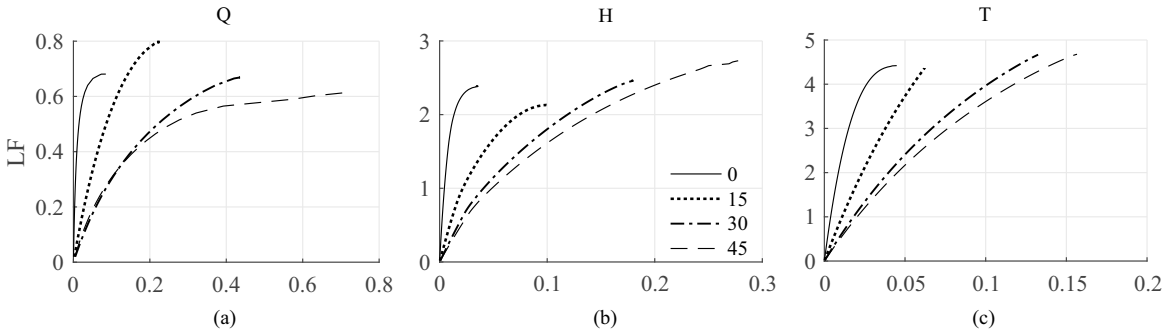

Figure 8: Load-displacement curves for each pattern and orientation angle

The sensitivity to the grid orientation of each gridshell layout is better highlighted in Figure 6, which plots for each analysis and layout the percentage variation of the load factor with respect to the reference configuration $\theta = 0°$:

$$\Delta\text{LF} = \frac{\text{LF}_i - \text{LF}_0}{\text{LF}_0}, \; i = 15, 30, 45. \tag{2}$$

The LF variations induced by the change in grid orientation with respect to the boundary structure are less pronounced and in some cases negligible for the isotropic gridshells (between ± 20%), but are significant for the orthotropic one, where they can amount to more than 40% for both LBA and GMNIA. In most cases, the orientation $\theta = 30°$ corresponds to the lowest variations of the load factor ($|\Delta\text{LF}| < 10\%$).

The buckling shapes (Figure 7) are strongly affected by the grid to boundary structure relative orientation, whichever the layout and the type of analysis. In general, the buckling shapes for each grid topology agree with what already observed by Malek *et al.* [17]: the grid pattern characterised by higher in-plane shear stiffness, *i.e.* the T pattern, shows local buckling, characterised by dimples, while the Q pattern, which has the lowest in-plane shear stiffness, displays global buckling with high wavelength. H gridshell displays an intermediate buckling behaviour, that could be defined as global with low wavelength (at least for LBA and GMNIA). Focusing on GMNA, the most significant effect of the rotation of the boundary structure with respect to the grid directions is to induce non-symmetrical collapse shapes also when the perfect structure is considered. Moreover, when the boundary structure is aligned with the grid direction, the node with maximum displacement (red circle) is usually located near the rigid boundary, while it moves in proximity of the free edge for $\theta \neq 0°$ (from "shell-driven" to "boundary-driven" collapse [31]).

5.2 Mechanical reading through Structural Eigen-stiffness

In this section, a deeper insight into the interpretation of the results of non linear analyses is provided. The mechanical reading proposed in the following is limited to the results of GMNA. This choice is given by the fact that the imperfection shape adopted in GMNIA (*i.e.* the first buckling shape from LBA) depends on the design variable θ and is, therefore, different for each analysed gridshell. This means that the effects of imperfection cumulate with and noise the effects induced by the variation of θ. Since the objective of this study is to focus on the effects of anisotropy, the latters can be better isolated and interpreted by referring to the perfect geometry.

Figure 8 plots the load-displacement curves referred to the node of maximum displacement for each layout. Some general qualitative trends can be identified: the T pattern is the one corresponding to the highest stiffness and to the lowest displacements at the ultimate state, in opposition to the Q pattern [18]; for all the patterns, the increase in θ corresponds to a decrease in the initial slope of the load-displacement curve and an increase in softening (*i.e.* in the ultimate displacement).

In order to have a more synthetic quantification of these effects, the results of GMNA are analysed through the concept of Structural Eigen-stiffness (SES), introduced by Zhu *et al.* [39]. The Eigen-stiffness is a scalar quantity that provides a measure of the global structural stiffness. The basic theory for deriving SES is herein briefly recalled. For further details the reader can refer to the original paper [39].

Considering the generic j-th iteration step of a non linear structural analysis, the SES is defined as:

$$k_j^\star = \frac{\Delta\mathbf{U}_j^T \mathbf{K}_{\text{T}j} \Delta\mathbf{U}_j}{\Delta\mathbf{U}_j^T \Delta\mathbf{U}_j} = \frac{\Delta p_j^\star}{\Delta u_j^\star}, \tag{3}$$

where $\Delta\mathbf{U}_j$ is the incremental displacement vector and $\mathbf{K}_{\text{T}j}$ is the tangent stiffness matrix at step j; $\Delta u_j^\star$ and $\Delta p_j^\star$ are

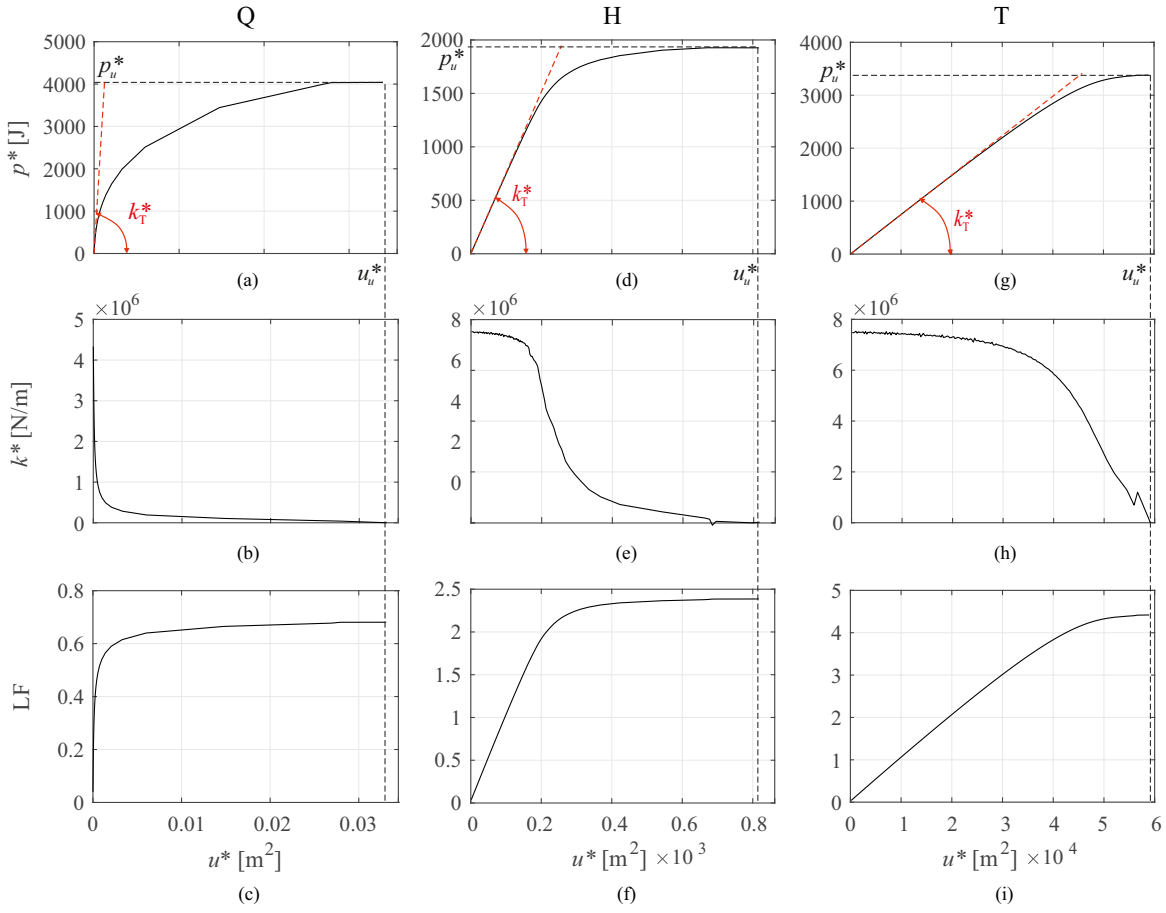

Figure 9: Structural Eigen-curves for Q, H and T gridshells with $\theta = 0$

the incremental Eigen-displacement and incremental work, respectively, defined as:

$$\Delta u_j^\star = \Delta \mathbf{U}_j^T \Delta \mathbf{U}_j, \tag{4}$$

$$\Delta p_j^\star = \Delta \mathbf{U}_j^T \Delta \mathbf{P}_j, \tag{5}$$

where $\Delta \mathbf{P}_j$ is the incremental load vector. The SES has the same dimension as the structural stiffness and it equals the work done by incremental load $\Delta \mathbf{P}$ on the condition of $\Delta u^\star = 1$.

The advantage of computing SES is that it does not rely on a specific nodal displacement, but it takes into account the displacements of all nodes. This is particularly useful in a comparative study, where it would be almost impossible to chose the same representative node for all the design solutions to evaluate load-displacement curves. Indeed, the node with maximum displacement, usually adopted as reference node, is different for each analysed gridshell.

An example of Structural Eigen-curves is reported in Figure 9 for the three gridshells and $\theta = 0°$. The curves in the first row (Figures 9a-d-g) plots the cumulated incremental work $p^\star = \sum_{j=1}^{n} \Delta p_j^\star$ over the total number of steps n versus the cumulated incremental Eigen-displacement $u^\star = \sum_{j=1}^{n} \Delta u_j^\star$. The slope of the $p^\star - u^\star$ curve at each step j is the SES $k^\star$, plotted in Figures 9b-e-h versus $u^\star$. Finally, Figures 9c-f-i report the LF versus $u^\star$. It can be observed that $k^\star$ decreases as $u^\star$ increases and becomes null when the limit point is reached.

The tangent SES $k_T^\star$, evaluated as the slope of the $p^\star - u^\star$ curve at the origin, is calculated for each grid pattern and orientation angle and plotted in Figure 10. This allows to evaluate the effect of the boundary structure orientation on the initial global stiffness of the structure. The following considerations can be outlined:

- as expected, T gridshells have the highest global stiffness, while Q gridshells the lowest one;
- for all grid patterns, the initial global stiffness significantly decreases when the boundary structure is rotated with respect to the grid main directions;
- the Q gridshell is the most sensitive to the free edge orientation. When the free edge is not aligned with one of the grid main directions, the initial stiffness is reduced of around 95%.

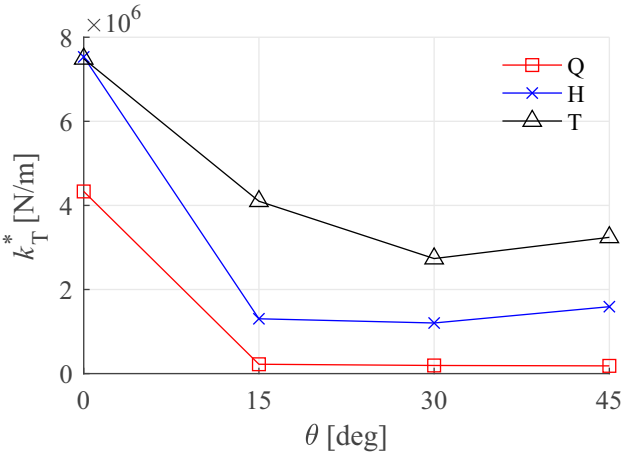

Figure 10: Tangent SES versus θ for each layout

The significant reduction of the initial global structural stiffness with respect to the original configuration $\theta = 0°$ is not reflected in a corresponding significant variation of the load factors. If the free edge orientation doesn't have a relevant influence on the gridshell ultimate behaviour, at least for isotropic gridshells, on the other hand the reduction of the initial stiffness when the free edge is not aligned with the grid directions is expected to have a significant influence on the structural behaviour in service. This is shown in Table 1, which reports the maximum displacements for each layout in service load condition, corresponding to a uniform load equal to $q_d + q_s$. It can be observed that, for all the considered patterns, the maximum displacement increases for increasing θ: this could lead to unacceptable displacements at the Serviceability Limit State (SLS) for some layouts. Note that bold values refer to layouts where the buckling load is lower than the SLS load, meaning that the reported displacement corresponds to the collapse one.

Table 1: Maximum displacement [mm] at the Serviceability Limit State

	0°	15°	30°	45°
Q	**84.7**	153	**433.2**	**720.5**
H	2.9	13.8	24.9	29.5
T	2.7	7.6	12.4	13.9

The results of this investigation lead to the following concluding remarks:

- isotropic gridshells have a low sensitivity to the orientation of the boundary structure in terms of Load Factor. The preferred orientation seems to coincide with $\theta = 0°$, which corresponds to the highest initial global stiffness of the structure and to the lowest in service displacements;
- orthotropic gridshells are highly sensitive to the orientation of the boundary structure both in terms of LF and initial stiffness. In this case, the best orientation should be carefully evaluated by considering the best compromise between, on one hand, the increase in LF and, on the other hand, the significant reduction of the initial structural stiffness, which could lead to unacceptable displacements in service conditions.

6 Conclusions

The presented study aimed at exploring the effects of anisotropy on the structural behaviour of free-edge gridshells. In fact, gridshells can be considered as discrete shells, and their behaviour differs from the one of continuous shells the more the grid topology approximation is far from the continuous isotropic shell. Therefore, the orientation of the grid with respect to the free-edges is expected to play a non negligible role in the stability of this kind of structures.

The study has been conducted by adopting as benchmark an ideal single-layer steel free-edge gridshell. Three different grid topologies have been considered, *i.e.*, quadrangular, hybrid and triangular. On the basis of the continuum analogy, the quad pattern can be classified as orthotropic, while the triangular pattern is the one which better approximate the behaviour of an isotropic shell. For each grid layout, four different orientations of the trimming vertical plane with respect to the grid directions have been analysed. The load factor and buckling shape have been calculated in each configuration by means of three structural analyses: linear buckling analysis (LBA) on the perfect geometry, geometrically and materially nonlinear analysis on both the perfect (GMNA) and imperfect structure (GMNIA). In the last case, the imperfection shape has been set as the first buckling mode shape scaled to $L/300$. A deeper insight into the influence of the grid orientation on the non linear behaviour of perfect gridshells has been provided through the concept of Structural Eigen-stiffness.

The results of the parametric study allow to draw the following concluding remarks:

- the change in grid orientation with respect to the boundary structure can induce non negligible variations of the load factors, which can reach 45% for some grid patterns and some values of the orientation angle θ. The variations of LF with respect to the

reference configuration $\theta = 0^\circ$ are more pronounced when geometrical imperfections are taken into account;
- when considering the perfect geometry, a significant reduction of the global structural initial stiffness can be observed if the boundary structure is not aligned with one of the main grid directions. Even though this stiffness reduction seems to have not a role in the ultimate structural behaviour, it should be seriously considered since it could lead to unacceptable displacements in service conditions;
- in summary, orthotropic and isotropic patterns display a different sensitivity to the grid orientation with respect to the boundary structure. Orthotropic gridshells, whose buckling load is mainly influenced by the in-plane shear stiffness, are the most sensitive to variation of the angle θ, both in terms of LF, of global structural stiffness and of softening before buckling. The opposite holds for isotropic gridshells, which result almost insensitive to the change in boundary structure orientation in terms of LF and for which the reference orientation $\theta = 0^\circ$ seems to be the most effective one.

These results, despite relative to a specific geometrical and structural set-up, suggest the need, in the design phase of a free-edge gridshell, to explore different grid orientation with respect to the boundary structure in order to identify the one corresponding to the most satisfying structural behaviour. The latter does not necessarily correspond to the case with highest buckling load, since also the reduction of the initial structural stiffness should be considered to avoid unacceptable in service displacements. In the case of more complex geometries than the one herein adopted as case study, *e.g.* free-form gridshells with multiple free-edges, this aim could be achieved by means of topology optimisation [36, 40, 41].

Funding information: The authors state no funding involved.

Author contributions: All authors have accepted responsibility for the entire content of this manuscript and approved its submission.

Conflict of interest: The authors state no conflict of interest.

References

[1] Schlaich J, Bergermann R. Leicht Weit/Light Structures. Berlin; 2004.
[2] Adriaenssens S, Barnes M. Tensegrity spline beam and grid shell structures. Eng Struct. 2001;23(1):29–36.
[3] Fraddosio A, Pavone G, Piccioni M. Minimal mass and selfstress analysis for innovative v-expander tensegrity cells. Compos Struct. 2019;209:754–74.
[4] Lewis W. Tension Structures: Form and Behaviour. London; 2017.
[5] Beckh M, Barthel R., The first doubly curved gridshell structure -Shukhovs building for the plate rolling workshop in Vyksa. In: Proc 3rd Int Congress Constr History. Cottbus; 2009.
[6] Fuller R, Ward J. The artifacts of R. Buckminster Fuller: a comprehensive collection of his designs and drawings. Garland; 1985.
[7] Liddell I., Frei Otto and the development of gridshells. Case Stud Struct Eng. 2015;4(2015):39–49.
[8] Schlaich J, Schober H. Glass-covered grid-shells. Struct Eng Int. 1996;6(2):88–90.
[9] Schober H. Transparent Shells: Form, Topology, Structure. John Wiley & Sons; 2015. https://doi.org/10.1002/9783433605998.
[10] Chilton J, Tang G. Timber Gridshells: architecture, structure and craft. Routledge; 2017.
[11] Rockwood D. Bamboo Gridshells. Routledge; 2015. https://doi.org/10.4324/9781315758343.
[12] Gioncu V. Buckling of reticulated shells: state-of-the-art. Int J Space Structures. 1995;10(1):1–46.
[13] IASS WG 8 for Metal Spatial Structures, (Draft) Guide to buckling load evaluation of metal reticulated roof structures. Tech. Rep. Int Assoc Shell Spatial Struct; 2014.
[14] Bulenda T, Knippers J. Stability of grid shells. Comput Struc. 2001;79(12):1161–74.
[15] Cai J, Gu L, Xu Y, Feng J, Zhang J. Nonlinear stability analysis of hybrid grid shells. Int J Struct Stab Dyn. 2013;13(1):1–16.
[16] Fan F, Cao Z, Shen S. Elasto-plastic stability of single-layer reticulated shells. Thin-walled Struct. 2010;48(10-11):827–36.
[17] Malek S, Wierzbicki T, Ochsendorf J. Buckling of spherical cap gridshells: A numerical and analytical study revisiting the concept of the equivalent continuum. Eng Struct. 2014;75(15):288–98.
[18] Tonelli D, Pietroni N, Puppo E, Froli M, Cignoni P, Amendola G, et al. Stability of statics aware Voronoi grid-shells. Eng Struct. 2016;116:70–82.
[19] Mesnil R, Douthe C, Baverel O, Léger B. Linear buckling of quadrangular and kagome gridshells: A comparative assess-ment. Eng Struct. 2017;132:337–48.
[20] Kato S, Mutoh I, Shomura M. Collapse of semi-rigidly jointed reticulated domes with initial geometric imperfections. J Construct Steel Res. 1998;48(2-3):145–68.
[21] Guo J. Research on distribution and magnitude of initial geometrical imperfection affecting stability of suspen-dome. Adv Steel Constr. 2011;7(4):344–58.
[22] Bruno L, Sassone M, Venuti F. Effects of the equivalent geometric nodal imperfections on the stability of single layer grid shells. Eng Struct. 2016;12:184–99.
[23] López A, Puente I, Serna MA. Direct evaluation of the buckling loads of semi-rigidly jointed single-layer latticed domes under symmetric loading. Eng Struct. 2007;29(1):101–9.

[24] Hwang KJ, Knippers J, Park SW. Influence of various types node connectors on the buckling loads of grid shells. In: Proc IASS Symp. Valencia, Spain; 2009.
[25] Ma H, Fan F, Wen P, Zhang H, Shen S. Experimental and numerical studies on a single-layer cylindrical reticulated shell with semi-rigid joints. Thin-walled Struct. 2015;86:1–9.
[26] Douthe C, Baverel O, Caron J. Gridshell in composite materials: towards wide span shelters. J. IASS. 2007;48(3):175–80.
[27] Williams C. The analytical and numerical definition of the geometry of the British Museum Great Court roof. In: Deakin University (Ed.). Math Design. Geelong, Australia; 2001.
[28] Happold E, Liddell W. Timber lattice roof for the Mannheim Bundesgartenschau. Struct Eng. 1975;53(3):99–135.
[29] Glymph J, Shelden D, Ceccato C, Mussel J, Schober H. A parametric strategy for free-form glass structures using quadrilateral planar facets. Autom Construct. 2004;13(2):187–202.
[30] Schober H, Justi S. Cabot Circus, Bristol – Ebene Viereckne tze für freigeformte glasdächer. Stahlbau. 2012;81 Supplement S1:28–42.
[31] Venuti F, Bruno L. Influence of in-plane and out-of-plane stiffness on the stability of free-edge gridshells: A parametric analysis. Thin-walled Struct. 2018;131:755–68.
[32] Cai J, Xu Y, Feng J, Zhang J. Nonlinear stability of a single-layer hybrid grid shell. J Civ Eng Manag. 2012;18(5):752–60.
[33] JGJ61-2003, Technical specification for reticulated shells (in Chinese). Standard, China Architect Ind Press. Beijing, China; 2010.
[34] Liuti A, Pugnale A, D'Amico B. Building timber gridshells with air: Numerical simulations and technique challenges. In: Proc 3rd Int Conf Struct Architect (ICSA2016). Structures and Architecture: Beyond their Limits. Guimarães, Portugal; 2016.
[35] Pietroni N, Tonelli D, Puppo E, Froli M, Scopigno R, Cignoni P. Statics aware grid shells. Comput Graph Forum. 2015;34(2):627–41.
[36] Winslow P, Pellegrino S, Sharma S. Multi-objective optimization of free-form grid structures. Struct Multidiscipl Optim. 2010 Jan;40(1-6):257–69.
[37] Wang D, Abdalla M. Buckling analysis of grid-stiffened composite shells. In: Marcal P, Yamagata N, (Eds). Design and Analysis of Reinforced Fiber Composites. Cham: Springer; 2016. https://doi.org/10.1007/978-3-319-20007-1_1.
[38] Lebée A, Sab K. Homogenization of a space frame as a thick plate: application of the bending-gradient theory to a beam lattice. Comput Struc. 2013;127:88–101.
[39] Zhu ZC, Luo YF, Xiang Y. Global stability analysis ofspatial structures based on eigen-stiffness and structural eigen-curve. J Construct Steel Res. 2018;141:226–40.
[40] Richardson J, Adriaenssens S, Coelho R, Bouillard P. Coupled form-finding and grid optimization approach for single layer grid shells. Eng Struct. 2013;52:230–9.
[41] Oval R, Rippmann M, Mesnil R, Mele TV, Baverel O, Block P. Feature-based topology finding of patterns for shell structures. Autom Construct. 2019;103:185–201.